Cancer Research

Identification of Tumorigenic Cells in *Kras*^{G12D}-Induced Lung Adenocarcinoma

Huan-Chieh Cho[1,2], Chao-Yang Lai[2], Li-En Shao[2], and John Yu[2,3]

Abstract

We established an inducible *Kras*^{G12D}-driven lung adenocarcinoma in *CCSP-rtTA/TetO-Cre/LSL-Kras*^{G12D} mice that enable pursuits of the cellular and molecular processes involved in *Kras*-induced tumorigenesis. To investigate the cellular origin of this cancer, we first report a strategy using fluorescence-activated cell sorting fractionation that could highly enrich bronchiolar Clara and alveolar type II cells, respectively. The EpCAM^{+}MHCII^{-} cells (bronchiolar origin) were more enriched with tumorigenic cells in generating secondary tumors than EpCAM^{+}MHCII^{+} cells (alveolar origin) in primary tumors that had been already initiated with oncogenic *Kras* activation. In addition, secondary tumors derived from EpCAM^{+}MHCII^{-} cells showed diversity of tumor locations compared with those derived from EpCAM^{+}MHCII^{+} cells. In the alveolar region, secondary tumors from EpCAM^{+}MHCII^{-} cells expressed not only bronchiolar epithelial marker, panCK, but also differentiation marker, proSPC, consistent with the notion that cancer-initiating cells display not only the abilities for self-renewal but also the features of differentiation to generate heterogeneous tumors with phenotypic diversity. Furthermore, high level of ERK1/2 activation and colony-forming ability as well as lack of Sprouty-2 expression were also observed in EpCAM^{+}MHCII^{-} cells. Therefore, these results suggest that bronchiolar Clara cells are the origin of cells and tumorigenesis for *Kras*^{G12D}-induced neoplasia in the lungs. *Cancer Res; 71(23); 7250–8. ©2011 AACR.*

Introduction

Lung cancer is the leading cause of cancer-related mortality worldwide (1). Constitutive activation of the *Kras* oncogene was found in 20% to 40% of non–small-cell lung cancer, about 80% of which occurred at codon 12 (2). *Kras* encodes a small GTPase that mediates a wide range of cellular functions, including proliferation, apoptosis, cytoskeletal remodeling, and differentiation (3). There are primarily 2 major types of effector proteins: Rafs and phosphoinositide 3-kinase (PI3K). Raf serine/threonine kinases phosphorylate and activate mitogen-activated protein kinase kinases (MEK1/2), which in turn phosphorylate and activate extracellular signal–regulated kinases (ERK1/2; ref. 4). However, Sprouty-2 is an antagonist of Raf kinases that suppresses Ras–MEK–ERK signaling activation and tumorigenesis in *Kras*^{G12D}-mediated lung cancer (5, 6). In addition, the PI3K–Akt pathway is an essential cell survival pathway and cooperates with activated Raf to cause synergistic transforming activity (7). Furthermore, Ras-dependent malignant transformation required the activation of Stat3 pathway (8).

Different regions of resident stem/progenitor cells are responsible for lung postnatal growth, homeostasis, and repair of injured lungs, and contribute to local needs in times of tissue damage (9). The Oct-3/4 positive lung stem/progenitor cells residing in the terminal bronchiolar region of neonatal lungs have been shown to be susceptible to SARS-CoV infection (10). In addition, bronchioalveolar stem cells that reside in the bronchioalveolar junction of adult lungs express both Clara cell secretion proteins (CC10) and prosurfactant protein-C protein (proSPC), which are respective markers for bronchiolar Clara cells and alveolar type II cells (11). Furthermore, other group have also identified rare population of lung epithelial stem/progenitor cells with the capacity for self-renewal and that give rise to airway and alveolar epithelial cell lineages *in vitro* (12). Taking these results together, there is no direct evidence that these lung stem/progenitor cells are the sole inducer of bronchiogenic carcinomas of lungs. However, these studies may imply that tumorigenic cells or tumor-initiating cells of lung may be derived from bronchiolar Clara cells.

Identification of the cell origin of lung adenocarcinomas and defining the biochemical and biological changes that accompany their transformation are essential for the development of early detection and treatment. In this study, we first described the use of 3 surface markers, EpCAM, MHCII, and ICAM1, to enrich bronchiolar ciliated, Clara, and alveolar type II cells from normal lungs and *Kras*^{G12D}-induced malignancies, investigated the cellular origin of lung adenocarcinomas, and

Authors' Affiliations: [1]Institute of Microbiology and Immunology, National Yang-Ming University; and [2]Genomics Research Center and [3]Institute of Cellular and Organismic Biology, Academia Sinica, Taipei, Taiwan

Note: Supplementary data for this article are available at Cancer Research Online (http://cancerres.aacrjournals.org/).

Corresponding Author: John Yu, Genomics Research Center and Institute of Cellular and Organismic Biology, Academia Sinica, 128 Academia Rd., Sec. 2, Nankang, Taipei 115, Taiwan. Phone: 886-2-2789-9500; Fax: 886-2-2789-9588; E-mail: jyu@gate.sinica.edu.tw

doi: 10.1158/0008-5472.CAN-11-0903

determined the molecular processes that may be involved in *Kras*-induced tumorigenesis.

Materials and Methods

Mice

The conditional mutant mice are described in the Supplementary Materials and Methods.

Fluorescence-activated cell sorting analysis of total lung cells

Single-cell suspension prepared from lung tissues of the mice are described in the Supplementary Materials and Methods. It was found that the total number of lung cells was approximately $1.3 \times 10^7 \pm 0.2 \times 10^7$ (mean $\pm$ SD, $n = 5$) in the conditional mutant mice prior to $Kras^{G12D}$ activation. After $Kras^{G12D}$ activation for 12 weeks, the total number of lung cells recovered from mice was $7.6 \times 10^7 \pm 0.7 \times 10^7$ (mean $\pm$ SD, $n = 5$).

Tumor engraftment analysis

Primary tumor cells were dissected from conditional mutant mice, which had received doxycycline administration for 12 weeks as described. Then, cell suspensions were pipetted into 200 μL of Dulbecco's modified Eagle's medium containing 20% fetal calf serum and injected into nonobese diabetic-severe combined immunodeficient (NOD-SCID) mice intravenously. Hematoxylin and eosin (H&E)-stained sections of lung tumors of recipient mice were imaged on an Aperia microscope (Aperia Technologies) and stitched together using Snapshot software to measure the tumor number and size (diameter). Percentages of $Ki76^+$ and $pERK1/2^+$ cells in secondary tumor areas were determined using MetaMorph software (Molecular Devices).

Immunofluorescence and immunohistochemical staining

The procedures of staining are described in the Supplementary Materials and Methods.

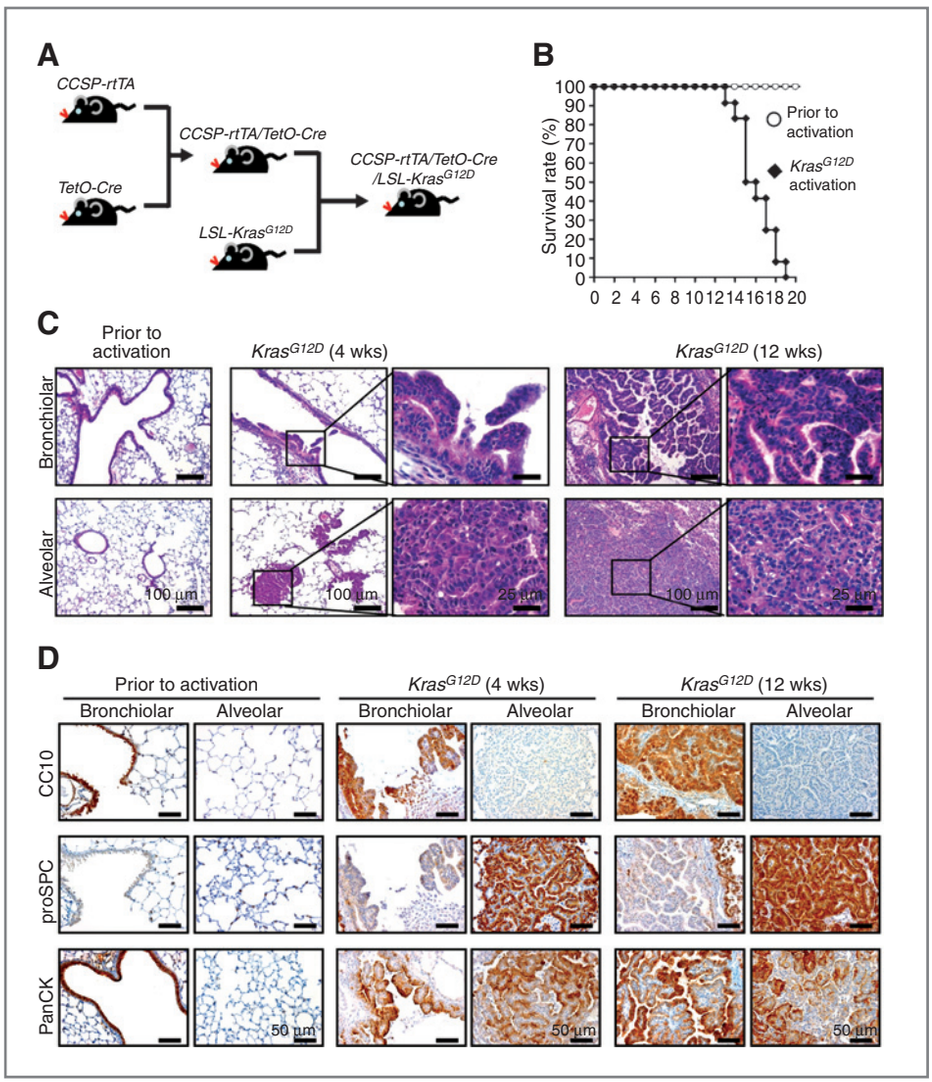

Figure 1. Immunohistochemical analysis of normal lung and $Kras^{G12D}$-induced lung lesions. A, lung epithelial cell–specific *CCSP-rtTA* mouse strain was crossed with the inducible *TetO-Cre* mouse strain to obtain *CCSP-rtTA/TetO-Cre* mice that were further crossed with *LSL-*$Kras^{G12D}$ knock-in mice to obtain *CCSP-rtTA/TetO-Cre/LSL-*$Kras^{G12D}$ conditional mutant mice. B, the Kaplan–Meier survival curve is shown for conditional mutant mice in response to the absence or presence of doxycycline, $n = 12$. C, H&E-stained tissue sections from conditional mutant mice prior to and after $Kras^{G12D}$ activation for 4 and 12 weeks. D, lung tissues from mice prior to and after $Kras^{G12D}$ activation for 4 and 12 weeks stained with antibodies directed against CC10, proSPC, and panCK (a bronchiolar epithelial marker) in bronchiolar and alveolar regions are shown.

Western blot and gene expression analysis

The procedures of Western blot and semiquantitative reverse transcriptase PCR (RT-PCR) are described in the Supplementary Materials and Methods.

Colony-formation assay and measurement of cytokines

The colony-formation assay are described in the Supplementary Materials and Methods.

Statistical analysis

Student *t* test was used to analyze the results of the experiments, and the *P* value was considered to be significant at less than 0.05. Data are expressed as the mean ± SE.

Results

Induced *Kras^{G12D}* activation with CCSP promoter activity

CCSP-rtTA/TetO-Cre/LSL-Kras^{G12D} conditional mutant mice were generated by cross-breeding *CCSP-rtTA/TetO-Cre* and *LSL-Kras^{G12D}* mice (Fig. 1A). In these mice, the expression of Cre recombinase is controlled by the tetracycline operator (tetO), which can be activated by the reverse tetracycline transactivator (rtTA) in the presence of doxycycline. The rtTA transgene is driven by the rat *CCSP* promoter, which is active in Clara cells in bronchioles and type II cells in alveoli (13). In Fig. 1B, these mice displayed a shortened lifespan with a median survival of 15 weeks after *Kras^{G12D}* activation, which was induced by the administration of doxycycline.

In contrast to mice prior to *Kras^{G12D}* activation, 4 weeks of *Kras^{G12D}* activation led to the development of epithelial hyperplasia in bronchioles and adenoma formation along alveoli (Fig. 1C). After 12 weeks of *Kras^{G12D}* activation, these lung lesions had subsequently progressed to adenocarcinomas in both the bronchiolar and alveolar regions (Fig. 1C). However, the mutated *Kras* in our system was not expressed in tissues other than lungs after *Kras^{G12D}* activation (Supplementary Fig. S1A and B).

In mice prior to *Kras^{G12D}* activation, the bronchiolar epithelium was positive for CC10, but negative for proSPC, whereas the alveolar epithelium was positive for proSPC, but negative for CC10 (Fig. 1D). However, after 4 and 12 weeks of *Kras^{G12D}* activation, bronchiolar tumor was also positive for CC10, but negative for proSPC, whereas alveolar tumor was negative for CC10 but showed intensive staining for proSPC (Fig. 1D). Thus, this profile of expression in primary tumor located in both bronchiolar and alveolar regions was reminiscent of the findings in normal lung, reflecting the oncogenic activation of *Kras^{G12D}* because of the *CCSP* promoter activity.

Furthermore, in mice prior to *Kras^{G12D}* activation, the bronchiolar epithelium of lung tissue showed intensive staining for pan-cytokeratin (panCK), whereas alveolar epithelia were negative (Fig. 1D). After 4 and 12 weeks of *Kras^{G12D}* activation, epithelial hyperplasia or adenocarcinomas located in bronchiolar regions were positive for panCK staining; but, in contrast, only about half of the adenomas and adenocarcinoma cells in alveolar regions were focally positive for panCK staining (Fig. 1D). These results implied that the initiating cells of lung tumor in the alveolar region might be derived from panCK$^+$ bronchiolar epithelia.

Fluorescence-activated cell sorting fractionation of lung cells with lineage markers

It was previously reported that the bronchiolar epithelium of normal lungs expresses either EpCAM or ICAM1, whereas the alveolar type II cell expresses MHCII and ICAM1 (12, 14, 15). We found that the EpCAM and MHCII expression profiles among viable CD45$^-$ cells defined 4 subpopulations in samples obtained from normal lung tissue (P1–P4 in Fig. 2A). Then, EpCAM$^+$MHCII$^-$ and EpCAM$^+$MHCII$^+$ cells (P1 and P2) were further examined for ICAM1 expression. In the EpCAM$^+$MHCII$^-$ cell population (P1), the percentage of ICAM1$^-$ cells (P5) exceeded that of ICAM1$^+$ cells (P6; Fig. 2A). On the other hand, the EpCAM$^+$MHCII$^+$ cell population (P2) revealed only one major ICAM1$^+$ cell population (P6; Fig. 2A). In addition, immunofluorescence staining confirmed that the EpCAM$^+$MHCII$^-$ICAM1$^-$, EpCAM$^+$MHCII$^-$ICAM1$^+$, and EpCAM$^+$MHCII$^+$ICAM1$^+$ cell fractions were enriched with bronchiolar ciliated, bronchiolar Clara, and alveolar type II cells, because these cells mainly reacted with, antibodies against β-tubulin IV$^+$, CC10$^+$, and proSPC$^+$, respectively (Fig. 2B).

After *Kras^{G12D}* activation for 4 and 12 weeks, the EpCAM$^+$MHCII$^-$ cells was also separated into ICAM1$^-$ and ICAM1$^+$ cell populations (P5 and P6). However, it was found that ICAM1$^-$ cells (P5) were reduced, whereas ICAM1$^+$ cells (P6) had dramatically increased in the EpCAM$^+$MHCII$^-$ cell population (P1; Fig. 2C). On the other hand, the EpCAM$^+$MHCII$^+$ cells also mostly showed one major ICAM1$^+$ cell population (P6; Fig. 2C). The immunofluorescence staining showed that EpCAM$^+$MHCII$^-$ cells (P1) reacted well with antibodies against β-tubulin IV and CC10; however, numbers of β-tubulin IV$^+$ cells decreased and CC10$^+$ cells increased after *Kras^{G12D}* activation for 12 weeks compared with normal lungs (Fig. 2D; Supplementary Fig. S2A). In addition, both bronchiolar and alveolar tumors were negative for β-tubulin IV staining (Supplementary Fig. S2B). These findings indicated that bronchiolar Clara cells increased, but ciliated cells decreased as *Kras*-induced tumorigenesis progressed from normal to an adenocarcinoma. On the other hand, EpCAM$^+$MHCII$^+$ cells (P2) also reacted well with proSPC (Fig. 2D; Supplementary Fig. S2A), indicating that the actually alveolar type II cells had also increased as a consequence of oncogene activation. The expressions of other lineage-specific genes and putative stem cell markers (Sca1 and CD133; data not shown) of the fractionated EpCAM$^+$MHCII$^-$ and EpCAM$^+$MHCII$^+$ cells from primary tumors were also characterized (Supplementary Fig. S2C), which confirmed that the EpCAM$^+$MHCII$^-$ fraction was enriched with bronchiolar cells, whereas the EpCAM$^+$MHCII$^+$ fraction was with alveolar cells.

Tumorigenicity of different cell fractions of primary tumors

We also found that primary tumors could be serially engrafted into immunodeficient mice to generate secondary and tertiary tumors (Supplementary Fig. S3A). These

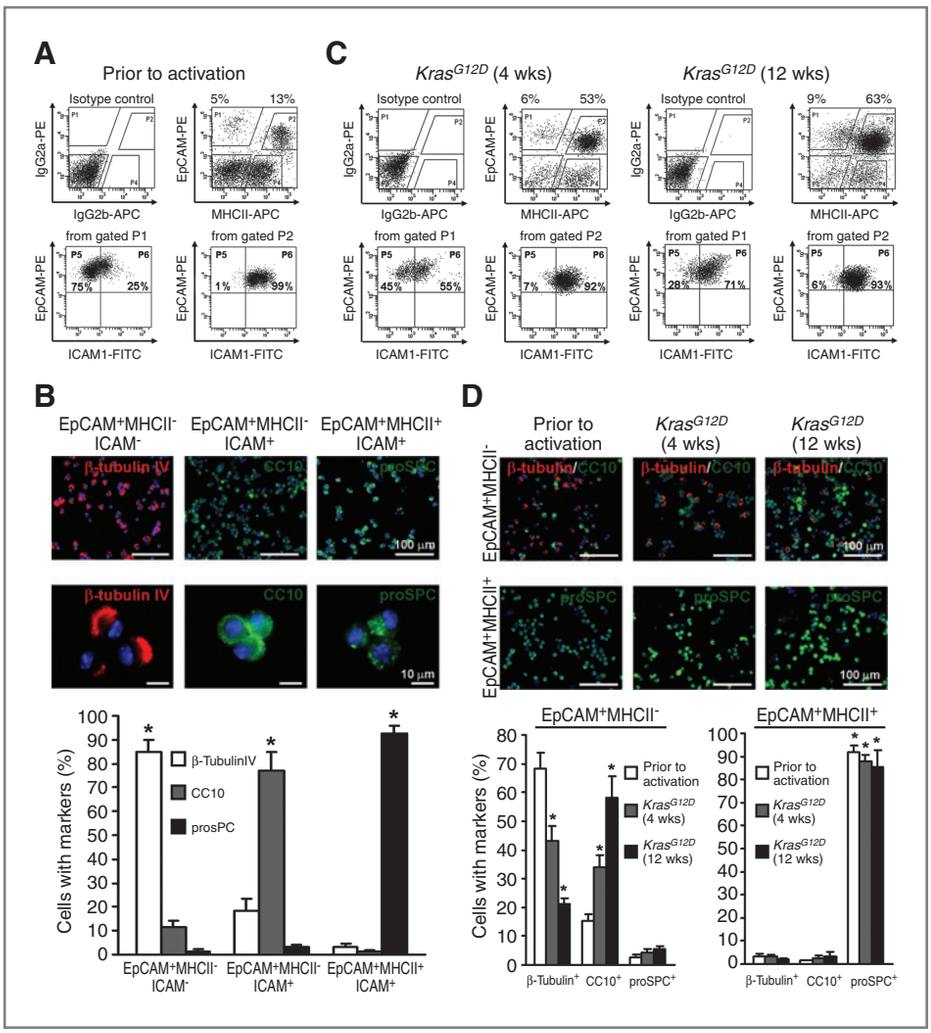

Figure 2. FACS and immunofluorescence analyses of cell fractions with lineage-specific markers. A, FACS analysis of CD45$^-$ lung cells prepared from mice prior to *Kras*^{G12D} activation. Representative dot plots of IgG isotype controls and expression profiles of EpCAM and MHCII CD45$^-$ cells are shown in the top row. ICAM1 expressions by EpCAM$^+$MHCII$^-$ (P1) and EpCAM$^+$MHCII$^+$ (P2) fractions are shown in the bottom row. B, immunofluorescence staining and quantification of the EpCAM$^+$MHCII$^-$ICAM1$^-$, EpCAM$^+$MHCII$^-$ICAM1$^+$, and EpCAM$^+$MHCII$^+$ICAM1$^+$ cell fractions stained with antibodies against β-tubulin IV (red), CC10 (green), and proSPC (green), respectively, and counterstained with 4′, 6-diamidino-2-phenylindole (DAPI; blue; mean ± SD, *, $P < 0.01$, $n = 5$, 2-tailed *t* test). C, FACS analysis of CD45$^-$ lung cells prepared from mice after *Kras*^{G12D} activation for 4 and 12 weeks. Representative dot plots of IgG isotype controls and expression profiles of EpCAM and MHCII CD45$^-$ cells are shown in the top row. ICAM1 expressions by the EpCAM$^+$MHCII$^-$ (P1) and EpCAM$^+$MHCII$^+$ (P2) fractions are shown in the bottom row. D, immunofluorescence staining and quantification of the EpCAM$^+$MHCII$^-$ cells (top row) double stained for β-tubulin IV (red) and CC10 (green), and EpCAM$^+$MHCII$^+$ cells (bottom row) stained for proSPC (green) and counterstained with DAPI (blue; mean ± SD, *, $P < 0.01$, $n = 3$, 2-tailed *t* test). FITC, fluorescein isothiocyanate.

secondary tumor cells were positive for ICAM1, but negative for *FoxJ1* (Supplementary Fig. S3B and C) and β-tubulin IV expression (data not shown). We then examined which fraction of the *Kras*^{G12D}-induced lung adenocarcinoma in primary tumors behave as cancer stem-like cells to generate secondary tumors, with not only the self-proliferation abilities but also displaying diversities in tumor locations, as well as phenotypic expression.

To compare tumorigenicity among different cell fractions, primary tumor cells after 12 weeks of *Kras*^{G12D} activation were fractionated into the EpCAM$^+$MHCII$^-$ (bronchiolar origin) and EpCAM$^+$MHCII$^+$ (alveolar origin) cells. These cells were, separately, injected intravenously into NOD-SCID mice. Twelve weeks after the injection, nodules of the secondary tumors that originated from the EpCAM$^+$MHCII$^-$ cell fraction were obviously larger (3.8-fold increase) and presented more tumor foci (6.5-fold increase) than tumor nodules originating from the EpCAM$^+$MHCII$^+$ cell fraction (Fig. 3A and B). In addition, the limiting dilution assay showed that a highly significant 6.6-fold enrichment for tumorigenic potential for EpCAM$^+$MHCII$^-$ cell fraction (Fig. 3C; Supplementary Table S1), compared with the EpCAM$^+$MHCII$^+$ cell fraction. Furthermore, secondary tumors derived from the injection of the EpCAM$^+$MHCII$^-$ cell fraction developed in both

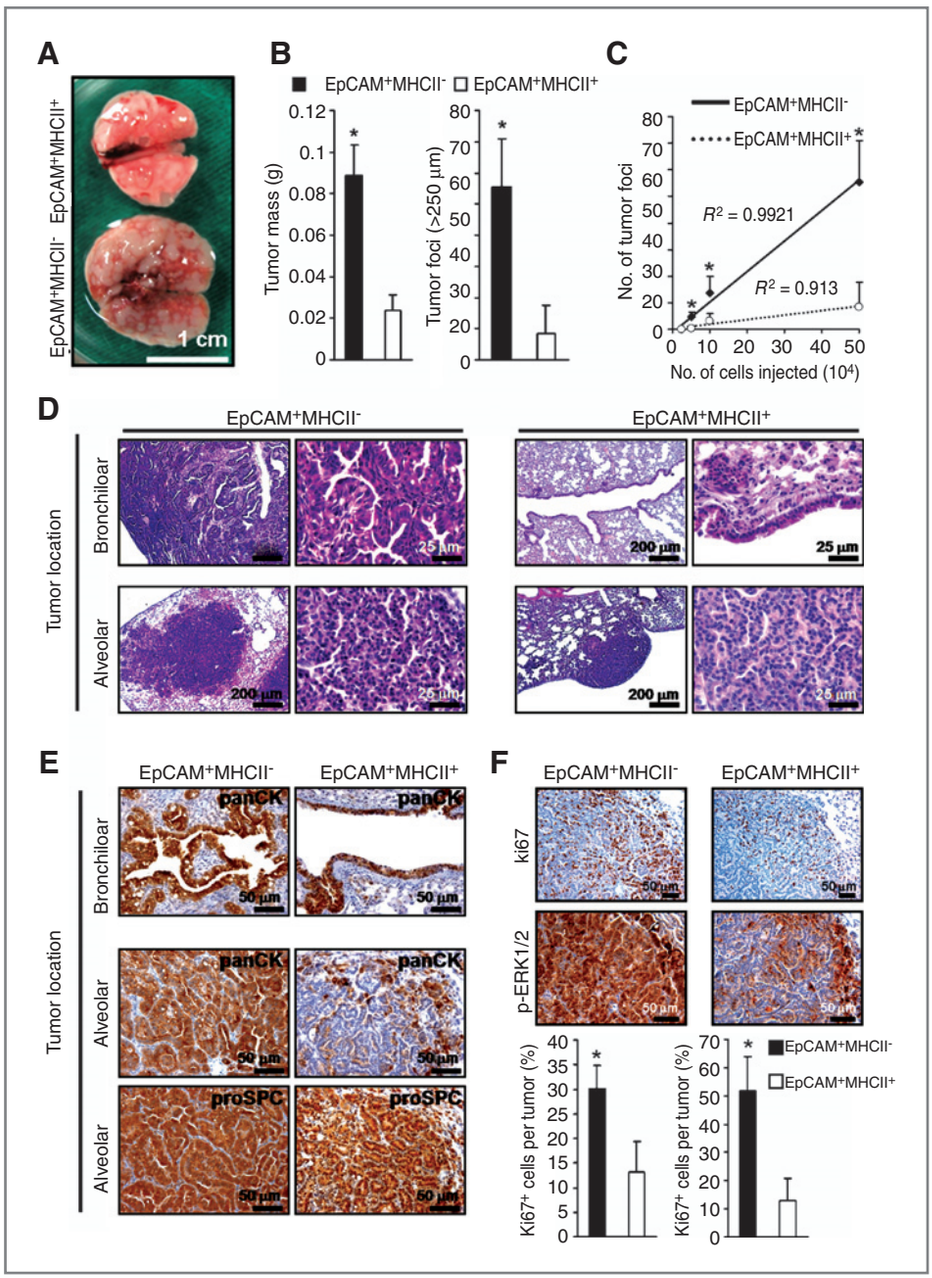

Figure 3. Tumorigenicity of EpCAM$^+$MHCII$^-$ and EpCAM$^+$MHCII$^+$ cell fractions from *Kras*^{G12D}-induced primary tumors. A, lung tissues were obtained from NOD-SCID mice injected with approximately 5×10^5 cells of the EpCAM$^+$MHCII$^-$ and EpCAM$^+$MHCII$^+$ fractions after *Kras*^{G12D} activation for 12 weeks. The lung lobes after injection of the EpCAM$^+$MHCII$^-$ cell fraction (left) were enlarged and showed multiple tumor foci compared with those injected with the EpCAM$^+$MHCII$^+$ cell fraction (right). B, comparison of tumor masses from mice injected with EpCAM$^+$MHCII$^-$ and EpCAM$^+$MHCII$^+$ cell fractions after subtraction of the nonengrafted lung weight. Numbers of tumor foci (>250 μm) in the engrafted lung tissue separately injected with the EpCAM$^+$MHCII$^-$ and EpCAM$^+$MHCII$^+$ cell fractions were counted on tissue sections (mean ± SD, *, $P < 0.01$, $n = 6$, 2-tailed *t* test; the number of mice used was presented in Supplementary Table S1). C, limiting dilution engraftment analysis of the tumorigenic potential of the EpCAM$^+$MHCII$^-$ (real line) and EpCAM$^+$MHCII$^+$ (dot line) tumor fractions (slopes: 1.13 vs. 0.17) are shown (mean ± SD, *, $P < 0.05$, 2-tailed *t* test; the number of mice used was presented in Supplementary Table S1). D, H&E staining of lung tissue sections obtained from mice separately injected with the EpCAM$^+$MHCII$^-$ and EpCAM$^+$MHCII$^+$ cell fractions. E, immunohistochemical analysis of lung tissue sections of secondary lung tumors stained for panCK or proSPC, which were separately injected with EpCAM$^+$MHCII$^-$ and EpCAM$^+$MHCII$^+$ cell fractions. F, immunohistochemical staining and quantification of Ki67$^+$ and phosphorylated ERK1/2$^+$ cells of secondary tumors separately injected with EpCAM$^+$MHCII$^-$ and EpCAM$^+$MHCII$^+$ cell fractions (mean ± SD, *, $P < 0.01$, $n = 6$, 2-tailed *t* test).

the bronchiolar and alveolar regions of recipient mice (Fig. 3D), whereas secondary tumors developed from the EpCAM$^+$MHCII$^+$ cell fraction occurred mainly in the alveolar region only, but not in the bronchiolar region (Fig. 3D). These results showed that the EpCAM$^+$MHCII$^-$-generated secondary tumors showed the diversity of tumor locations, whereas

the EpCAM$^+$MHCII$^+$ cells gave rise to tumors in the alveolar region because of the activated oncogenic *Kras*^{G12D}.

Phenotypic diversity of EpCAM$^+$MHCII$^-$-generated secondary tumors

The primary tumors in the bronchiolar region were positive for panCK staining, although about half of the primary tumors in the alveolar region were only focally positive for panCK staining (Fig. 1D). To test the hypothesis that panCK$^+$ tumors in the alveolar region might have been derived from the bronchiolar cell origin, we first examined which cell fraction in the normal and the primary tumors express panCK$^+$ tumors. As shown in Supplementary Fig. S4, most panCK$^+$ cells were found in the EpCAM$^+$MHCII$^-$ cell fraction of normal lungs, not in the EpCAM$^+$MHCII$^+$ cell fraction. However, after *Kras*^{G12D} activation for 12 weeks, only panCK$^+$, but not panCK$^+$proSPC$^+$ cells, were found in the EpCAM$^+$MHCII$^-$ cell fraction of the lung, whereas panCK$^+$proSPC$^+$ cells were observed in the EpCAM$^+$MHCII$^+$ cell fraction (Supplementary Fig. S4).

On the other hand, in the bronchiolar region, secondary tumors derived from the injection of the EpCAM$^+$MHCII$^-$ cell fraction were positive for panCK staining (Fig. 3E) that was consistent with the findings from primary tumors in the bronchiolar region (Fig. 1D). In addition, in the alveolar region, secondary tumors derived from the same cell fraction were also mostly positive for panCK; but also positive for proSPC staining (Fig. 3E). These results attested to the differentiation capacity of EpCAM$^+$MHCII$^-$ cells that were bronchiolar cells in origin, but apparently gave rise to panCK$^+$proSPC$^+$ tumors in the alveolar region. Furthermore, secondary tumors derived from EpCAM$^+$MHCII$^+$ cell fraction developed mainly in the alveolar region; these cells were rarely positive for panCK, but mostly positive for proSPC staining, which could be attributed to *Kras*^{G12D} activation (Fig. 3E).

Furthermore, staining for the mitotic marker Ki67 showed that there were a greater number of actively proliferating cells in secondary tumors derived from the EpCAM$^+$MHCII$^-$ cell fraction, but fewer proliferating cells in secondary tumors derived from the EpCAM$^+$MHCII$^+$ cell fraction (30% vs. 13% of Ki67$^+$ cells in Fig. 3F). This finding was consistent with the observation of larger tumor nodules in secondary tumors derived from the EpCAM$^+$MHCII$^-$ cell fraction (Fig. 3A–C).

The Kras signaling pathway

The downstream effectors of Kras signaling pathways, such as MEK1/2, ERK1/2, Akt, Stat3, and *miR-21* were required for *Kras*-driven lung adenocarcinoma and crucial for tumor maintenance after the establishment of sizeable tumors (16–18). It was found that these downstream regulators significantly increased after *Kras*^{G12D} activation (data not shown), compared with prior to activation. In contrast to mice prior to *Kras*^{G12D} activation, the EpCAM$^+$MHCII$^-$ and EpCAM$^+$MHCII$^+$ cell fractions expressed high levels of Kras RNA and protein after 12 weeks of *Kras*^{G12D} activation (Fig. 4A). The elevated *Kras* in both fractions was the mutated *Kras*^{G12D}, but not the inherent *Kras*^{G12D} after *Kras*^{G12D} activation (Supplementary Fig. S5A–C). In mice prior to *Kras*^{G12D} activation, the EpCAM$^+$MHCII$^-$ and EpCAM$^+$MHCII$^+$ cell fractions both expressed ERK1/2 proteins, but did not express phosphorylated ERK1/2 (Fig. 4B). In mice after *Kras*^{G12D} activation for 12 weeks, the EpCAM$^+$MHCII$^-$ cell fraction expressed significant amounts of phosphorylated ERK1 and ERK2 proteins (respectively, 24- and 37-fold) compared with the EpCAM$^+$MHCII$^+$ cell fraction, although both cell fractions expressed almost similar amounts of ERK1/2 proteins (Fig. 4B).

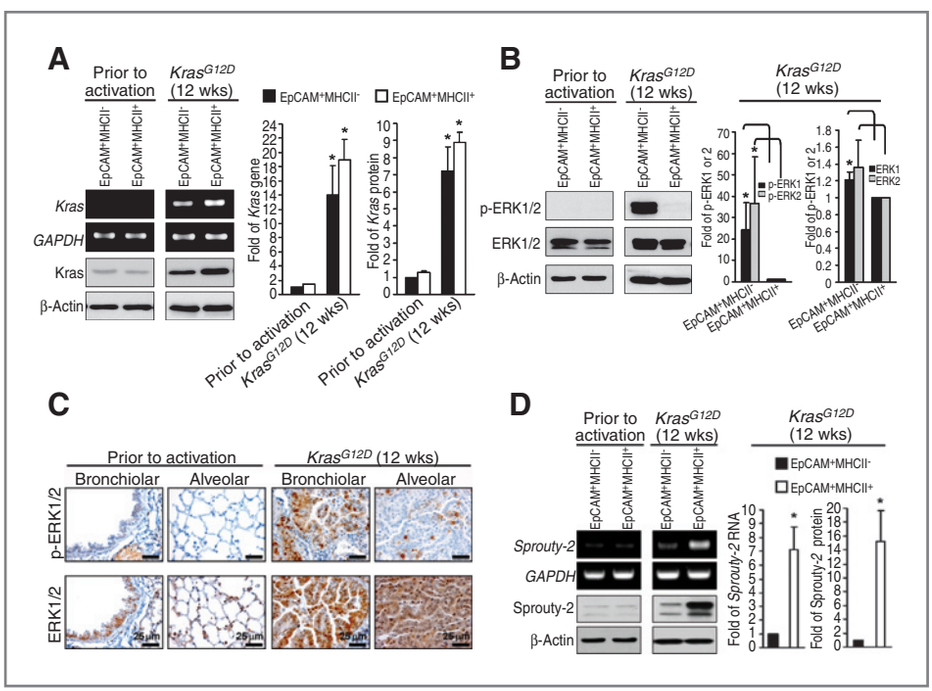

Figure 4. Activation profile of the Ras-ERK signaling pathway after *Kras*^{G12D} activation. A, RT-PCR and Western blot analyses of Kras RNA and protein expressions in EpCAM$^+$MHCII$^-$ and EpCAM$^+$MHCII$^+$ cell fractions from mice prior to and after *Kras*^{G12D} activation for 12 weeks. GAPDH and β-actin were used as internal controls (mean ± SD, *, $P < 0.05$, $n = 5$, 2-tailed *t* test). B, Western blot of phosphorylated ERK1/2, total ERK1/2, and β-actin in each cell fraction from mice prior to and after *Kras*^{G12D} activation for 12 weeks (mean ± SD, *, $P < 0.05$, $n = 5$, 2-tailed *t* test). C, immunohistochemical staining of lung tissue sections for phosphorylated ERK1/2 and total ERK1/2 expressions in bronchiolar and alveolar regions. D, RT-PCR and Western blot analyses of Sprouty-2 expressions (mean ± SD, *, $P < 0.01$, $n = 5$, 2-tailed *t* test). GAPDH, glyceraldehyde-3-phosphate dehydrogenase.

It was also found that phosphorylated ERK1/2$^+$ cells had obviously increased in primary bronchiolar tumors of the lungs after 12 weeks of *Kras*^{G12D} activation, whereas there were a few phosphorylated ERK1/2$^+$ cells scattered within the alveolar region (Fig. 4C). These findings were consistent with the staining pattern of phosphorylated ERK1/2 in EpCAM$^+$MHCII$^-$ cells (Fig. 4B). It was further found that secondary tumors derived from the EpCAM$^+$MHCII$^-$ cell fraction more highly expressed phosphorylated ERK1/2 compared with secondary tumors originating from the EpCAM$^+$MHCII$^+$ cell fraction (52% vs. 13% of p-ERK1/2$^+$ cells in Fig. 3F), indicating that the Kras signaling pathway were highly activated in the EpCAM$^+$MHCII$^-$ cell fraction.

On the other hand, the expression of Sprouty-2 was low in both the EpCAM$^+$MHCII$^-$ and EpCAM$^+$MHCII$^+$ cell fractions of mice prior to *Kras*^{G12D} activation (Fig. 4D). However, after 12 weeks of *Kras*^{G12D} activation, the expression levels of Sprouty-2 RNA and protein in the EpCAM$^+$MHCII$^+$ cell fraction, respectively, increased by 7- and 15-fold compared with those in the EpCAM$^+$MHCII$^-$ cell fraction (Fig. 4D). The expression pattern of Sprouty-2 was thus consistent with the lack of phosphorylated ERK1/2 in the EpCAM$^+$MHCII$^+$ cell fraction in the mice after 12 weeks of *Kras*^{G12D} activation (Fig. 4B). In addition, the gp130/Stat3 signaling pathway also highly activated in EpCAM$^+$MHCII$^-$ cells compared with EpCAM$^+$MHCII$^+$ cells after *Kras*^{G12D} activation for 12 weeks (data not shown). However, the expression level of phosphorylated Akt protein was not significantly changed between both fractions after *Kras*^{G12D} activation for 12 weeks (data not shown).

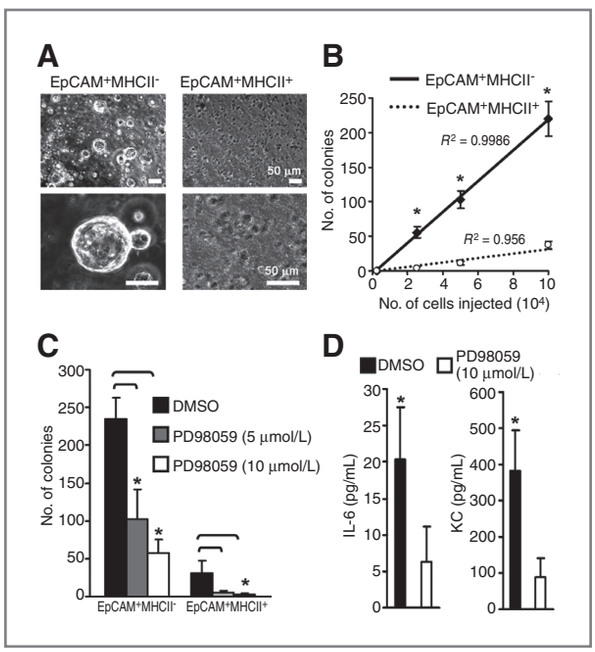

Figure 5. Colony-forming ability of EpCAM$^+$MHCII$^-$ and EpCAM$^+$MHCII$^+$ cells from *Kras*^{G12D}-induced primary tumors. A, phase-contrast photography of epithelial colonies obtained after 8 to 10 days of culture with 10^5 fractionated EpCAM$^+$MHCII$^-$ and EpCAM$^+$MHCII$^+$ tumor cells from mice after *Kras*^{G12D} activation for 12 weeks. B, a linear progression analysis of the cloning efficiency of the bronchiolar (real line) and alveolar (dot line) tumor fractions (slopes: 21.7 vs. 3.7) are shown (mean ± SD, *, $P < 0.01$, $n = 5$, 2-tailed *t* test). C, approximately 10^5 fractionated EpCAM$^+$MHCII$^-$ and EpCAM$^+$MHCII$^+$ tumor cells were seeded in the transwells. On day 0, the culture medium in the lower chamber was treated with dimethyl sulfoxide (DMSO), and 5 and 10 μmol/L of a MEK inhibitor (PD98059). After 8 to 10 days of culture, the colony number was counted by inverted microscopy (mean ± SD, *, $P < 0.05$, $n = 5$, 2-tailed *t* test). D, similarly, cells were seeded in transwells as in (C) and treated with DMSO and 10 μmol/L of MEK inhibitor (PD98059) in the lower chamber. After 2 days of culture, the conditioned medium in the lower chamber was collected, and cytokine production was assayed (mean ± SD, *, $P < 0.05$, $n = 3$, 2-tailed *t* test).

The efficiency of colony formation

The colony numbers from EpCAM$^+$MHCII$^-$ cells after 10 to 12 days of culture were significantly higher than those from EpCAM$^+$MHCII$^+$ cells (Fig. 5A). A linear analysis showed that the incidence of colony formation was directly proportional to the numbers of EpCAM$^+$MHCII$^-$ and EpCAM$^+$MHCII$^+$ cells seeded in the culture, and the colony-forming efficiency of EpCAM$^+$MHCII$^-$ cells substantially increased by 5.7-fold compared with EpCAM$^+$MHCII$^+$ cells (Fig. 5B), suggesting that EpCAM$^+$MHCII$^-$ cells contained a greater number of tumorigenic cells than did EpCAM$^+$MHCII$^+$ cells (Fig. 3A and B).

To determine whether ERK1/2 activation was involved in colony formation of tumor cells, the MEK inhibitor PD98059, which inhibits the phosphorylation of ERK1/2, was added to the culture medium of the lower chamber. After treatment of cells with PD98059 for 8 to 10 days, the colony numbers of EpCAM$^+$MHCII$^-$ cells had, respectively, decreased by 2.3- and 4.1-fold with 5 and 10 μmol/L inhibitors compared with the control (Fig. 5C), suggesting that the ERK signaling pathway

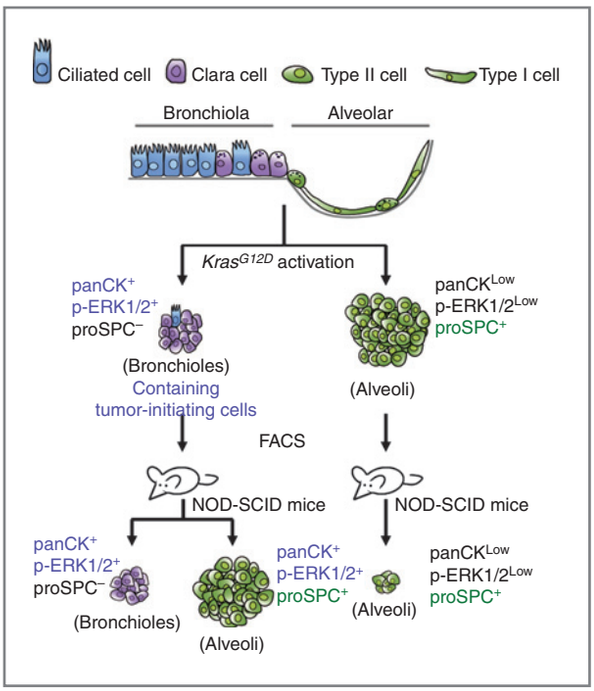

Figure 6. Primary bronchiolar tumor cells display the abilities for self-renewal and the capacity of differentiation to generate secondary tumors with phenotypic diversity, in contrast to alveolar tumor cells.

supported colony formation by EpCAM$^+$MHCII$^-$ cells. However, there was no significant difference in the colony numbers of EpCAM$^+$MHCII$^+$ cells treated with 5 μmol/L of PD98059; but 10 μmol/L of PD98059 significantly reduced colony formation by 9.8-fold (Fig. 5C).

It was noted that oncogenic *Ras* induced the secretion of the interleukin (IL)-6 and KC from a variety of cell types that mediate tumor growth and angiogenesis (19, 20), implying that these two cytokines are regulated by the Ras–MEK–ERK pathway. To test this hypothesis, cultured medium in the lower chamber from EpCAM$^+$MHCII$^-$ cells was collected after treatment with 10 μmol/L of PD98059 for 2 days and then cytokine production was determined. The production of IL-6 and KC from EpCAM$^+$MHCII$^-$ cells was blocked by PD98059 (by 3.2- and 5.8-fold) compared with the control (Fig. 5D), suggesting that the ERK signaling pathway was involved in IL-6 and KC secretion by EpCAM$^+$MHCII$^-$ cells.

Discussion

The bronchiolar adenocarcinomas and bronchoalveolar cell carcinomas of the peripheral airways are the most common types of lung cancer worldwide (21). These tumors might arise from Clara cells present in bronchioles or type II cells in alveoli (22, 23). However, the initiating cells in lung epithelium from which lung adenocarcinomas originate are poorly understood. Therefore, the identification of lung tumorigenic or tumor-initiating cells and their associated biomarkers or biosignatures will be useful for development of new detection methods and therapeutics for lung cancers. As illustrated in Fig. 6, the EpCAM$^+$MHCII$^-$ (bronchiolar origin) cells in the primary *Kras^{G12D}*-induced lung adenocarcinoma contained a significant amount of tumorigenic cells, as compared with the EpCAM$^+$MHCII$^+$ (alveolar origin) cells. Furthermore, EpCAM$^+$MHCII$^-$ cells generated secondary tumors, which displayed diversity of tumor locations, because they could give rise to tumors in both the bronchiolar and alveolar regions. In contrast, tumors derived from EpCAM$^+$MHCII$^+$ cells were located only in the alveolar region. On the basis of analysis with lineage markers, secondary tumors in the bronchiolar and alveolar regions generated from EpCAM$^+$MHCII$^-$ cells of primary tumor expressed panCK, suggesting that bronchiolar Clara cells are the origin of cells and tumorigenesis for *Kras^{G12D}*-induced neoplasia in the lungs.

On the other hand, secondary tumors derived from the EpCAM$^+$MHCII$^+$ fraction were mostly negative for panCK staining, suggesting these secondary tumors did not arise from bronchiolar cells. In other words, these secondary tumors developed from the EpCAM$^+$MHCII$^+$ fraction could be the consequence of oncogenic activation in *Kras^{G12D}* due to the *CCSP* promoter activity in the alveolar type II cells (13). Moreover, in addition to expression of panCK, secondary tumors in the alveolar region generated from bronchiolar EpCAM$^+$MHCII$^-$ cells were also positive for proSPC staining, similar to tumors derived from EpCAM$^+$MHCII$^+$ cells, suggesting that the tumorigenic cells from EpCAM$^+$MHCII$^-$ fraction also possessed the differentiation capacity to express the alveolar cell lineage marker.

The colony-forming ability of EpCAM$^+$MHCII$^-$ cells was significantly higher than that of EpCAM$^+$MHCII$^+$ cells, consistent with the observation that EpCAM$^+$MHCII$^-$ cells generated larger and more tumor foci than did EpCAM$^+$MHCII$^+$ cells. Furthermore, ERK1/2 highly activated in EpCAM$^+$MHCII$^-$ (bronchiolar origin) cells compared with EpCAM$^+$MHCII$^+$ (alveolar origin) cells after *Kras^{G12D}* activation for 12 weeks. In addition, the colony-forming ability of EpCAM$^+$MHCII$^-$ cells was reduced by treatment with the MEK inhibitor. These findings indicated that greater numbers of aggressive tumor cells or tumorigenic cells in the *Kras^{G12D}*-induced primary tumors were located in bronchiolar regions.

In this study, the EpCAM antigen was combined with MHCII and ICAM1 antigens to characterize and purify these cells and tumors in different regions in respective cell fractions by fluorescence-activated cell sorting (FACS) fractionation. Therefore, the development of lung lesions and different types of cancer progression after oncogenic activation could be monitored. Thus, this model might provide an efficient tool to examine signaling profiles of bronchiolar and alveolar tumors and analyze potential differential sensitivities of bronchiolar and alveolar tumors to conventional drugs and specific inhibitors.

Disclosure of Potential Conflicts of Interest

No potential conflicts of interest were disclosed.

Acknowledgments

The authors thank Dr. Chia-Ning Shen and Dr. Ruey-Jen Lin (Genomics Research Center, Academia Sinica) for helpful comments and experiments.

Grant Support

This study was supported by a grant from the National Science Council of Taiwan, NSC99-3111-B-001-006.

The costs of publication of this article were defrayed in part by the payment of page charges. This article must therefore be hereby marked *advertisement* in accordance with 18 U.S.C. Section 1734 solely to indicate this fact.

Received March 16, 2011; revised July 6, 2011; accepted September 28, 2011; published OnlineFirst November 16, 2011.

References

1. Samet JM, Avila-Tang E, Boffetta P, Hannan LM, Olivo-Marston S, Thun MJ, et al. Lung cancer in never smokers: clinical epidemiology and environmental risk factors. Clin Cancer Res 2009;15:5626–45.
2. Inoue A, Nukiwa T. Gene mutations in lung cancer: promising predictive factors for the success of molecular therapy. PLoS Med 2005;2:e13.
3. Downward J. Targeting RAS signalling pathways in cancer therapy. Nat Rev Cancer 2003;3:11–22.
4. Schubbert S, Shannon K, Bollag G. Hyperactive Ras in developmental disorders and cancer. Nat Rev Cancer 2007;7:295–308.
5. Kim HJ, Bar-Sagi D. Modulation of signalling by Sprouty: a developing story. Nat Rev Mol Cell Biol 2004;5:441–50.

6. Shaw AT, Meissner A, Dowdle JA, Crowley D, Magendantz M, Ouyang C, et al. Sprouty-2 regulates oncogenic K-ras in lung development and tumorigenesis. Genes Dev 2007;21:694–707.
7. Der CJ, Van Dyke T. Stopping ras in its tracks. Cell 2007;129: 855–7.
8. Gough DJ, Corlett A, Schlessinger K, Wegrzyn J, Larner AC, Levy DE. Mitochondrial STAT3 supports Ras-dependent oncogenic transformation. Science 2009;324:1713–6.
9. Rawlins EL, Okubo T, Xue Y, Brass DM, Auten RL, Hasegawa H, et al. The role of Scgb1a1 +Clara cells in the long-term maintenance and repair of lung airway, but not alveolar, epithelium. Cell Stem Cell 2009;4:525–34.
10. Ling TY, Kuo MD, Li CL, Yu AL, Huang YH, Wu TJ, et al. Identification of pulmonary Oct-4 +stem/progenitor cells and demonstration of their susceptibility to SARS coronavirus (SARS-CoV) infection in vitro. Proc Natl Acad Sci U S A 2006;103:9530–5.
11. Kim CF, Jackson EL, Woolfenden AE, Lawrence S, Babar I, Vogel S, et al. Identification of bronchioalveolar stem cells in normal lung and lung cancer. Cell 2005;121:823–35.
12. McQualter JL, Yuen K, Williams B, Bertoncello I. Evidence of an epithelial stem/progenitor cell hierarchy in the adult mouse lung. Proc Natl Acad Sci U S A 2010;107:1414–9.
13. Perl AK, Wert SE, Loudy DE, Shan Z, Blair PA, Whitsett JA. Conditional recombination reveals distinct subsets of epithelial cells in trachea, bronchi, and alveoli. Am J Respir Cell Mol Biol 2005;33:455–62.
14. Porter JC, Hall A. Epithelial ICAM-1 and ICAM-2 regulate the egression of human T cells across the bronchial epithelium. FASEB J 2009;23: 492–502.
15. Gereke M, Jung S, Buer J, Bruder D. Alveolar type II epithelial cells present antigen to CD4(+) T cells and induce Foxp3(+) regulatory T cells. Am J Respir Crit Care Med 2009;179:344–55.
16. Engelman JA, Chen L, Tan X, Crosby K, Guimaraes AR, Upadhyay R, et al. Effective use of PI3K and MEK inhibitors to treat mutant Kras G12D and PIK3CA H1047R murine lung cancers. Nat Med 2008;14:1351–6.
17. Tran PT, Fan AC, Bendapudi PK, Koh S, Komatsubara K, Chen J, et al. Combined Inactivation of MYC and K-Ras oncogenes reverses tumorigenesis in lung adenocarcinomas and lymphomas. PLoS One 2008;3: e2125.
18. Hatley ME, Patrick DM, Garcia MR, Richardson JA, Bassel-Duby R, van Rooij E, et al. Modulation of K-Ras-dependent lung tumorigenesis by MicroRNA-21. Cancer Cell 2010;18:282–93.
19. Ancrile B, Lim KH, Counter CM. Oncogenic Ras-induced secretion of IL6 is required for tumorigenesis. Genes Dev 2007;21:1714–9.
20. Karin M. Inflammation and cancer: the long reach of Ras. Nat Med 2005;11:20–1.
21. Minna JD, Roth JA, Gazdar AF. Focus on lung cancer. Cancer Cell 2002;1:49–52.
22. Meuwissen R, Berns A. Mouse models for human lung cancer. Genes Dev 2005;19:643–64.
23. Sutherland KD, Berns A. Cell of origin of lung cancer. Mol Oncol 2010;4:397–403.